Emergent Materials (2019) 2:79–93
https://doi.org/10.1007/s42247-018-0018-9

ORIGINAL ARTICLE

A brief overview of RF sputtering deposition of boron carbon nitride (BCN) thin films

Moustafa M. Zagho[1] · Hana D. Dawoud[1] · Nasr Bensalah[2] · T. M. Altahtamouni[1]

Received: 23 March 2018 / Accepted: 19 November 2018 / Published online: 30 November 2018

Abstract

A great part of interest has been paid for fabricating new materials with novel mechanical, optical, and electrical properties. Boron carbon nitride (BCN) ternary system was applied for variable bandgap semiconductors and systems with extreme hardness. The purpose of this literature review is to provide a brief historical overview of B_4C and BN, to review recent research trends in the BCN synthesizes, and to summarize the fabrication of BCN thin films by plasma sputtering technique from B_4C and BN targets in different gas atmospheres. Pre-set criteria are used to discuss the processing parameters affecting BCN performance which includes the gasses flow ratio and effect of temperature. Moreover, many characterization studies such as mechanical, etching, optical, photoluminescence, XPS, and corrosion studies of the RF sputtered BCN thin films are also covered. We further mentioned the application of BCN thin films to enhance the electrical properties of metal-insulator-metal (MIM) devices according to a previous report of Prakash et al. (Opt. Lett. **41**, 4249, 2016).

Keywords Radio frequency sputtering · Boron carbon nitride · Gas flow ratio · Metal-insulator-metal device

1 Introduction

1.1 Sputtering process

Sputtering technique is a physical vapor deposition technique that is considered a successful technique as a result of its features like a high film deposition rate and low-temperature structures [1]. It is a simple and economical method for producing thin films of alloys, metals, carbides, nitrides, and oxides [2]. The most common approach to this technique is the magnetron sputtering technique that uses a magnetic field to assist the process of depositing thin films onto a substrate. The particles (atoms and ions) are ejected through the transfer of momentum from the Ar ions. In a magnetron sputtering, electrons are confined along the magnetic field lines. A gaseous plasma that confines electrons is generated, and then accelerated to bombardment the target, which will lead to erode the material and eject them in the form of neutral particles and a minor component of ions. Inert gas is typically used as sputter gas like argon or even an active gas like nitrogen. Then, these ejected particles will place onto the substrate and coat a thin film of the target.

The magnetron sputtering technique offers great advantages compared with other techniques like uniform, homogeneity, and great adhesion deposition over the comparatively large area, facility to choose the substrate material and target material with very high melting points, high deposition rate, and also easy of the control of thickness [3]. However, several disadvantages of reactive sputtering for instance target poisoning, poor deposition rates, and arcing causing defects in the thin film [4]. From the other hand, there are main factors used to tune the thickness of the synthesized films in sputtering technique. These factors are the integrated pulse energy, deposition time, [5] chamber pressure, plasma gas, the angle of target and the substrate, and substrate temperature which is important to reduce the dopant redistribution and defect formation related to high-temperature processing [6].

Moustafa M. Zagho and Hana D. Dawoud contributed equally to this work.

Electronic supplementary material The online version of this article (https://doi.org/10.1007/s42247-018-0018-9) contains supplementary material, which is available to authorized users.

✉ T. M. Altahtamouni
taltahtamouni@qu.edu.qa

[1] Materials Science and Technology Program, College of Arts and Sciences, Qatar University, P. O. Box, 2713 Doha, Qatar

[2] Department of Chemistry and Earth Sciences, College of Arts and Sciences, Qatar University, P. O. Box, 2713 Doha, Qatar

However, different energy sources are required to maintain the plasma state in magnetron sputtering technique while it is losing power inside the chamber such as direct current (DC) for conductive targets for instance aluminum and copper, radio frequency (RF) for nonconductive targets like silicon and manganese dioxide, ion-beam sputtering which can depend only on an ion source without using any magnetic field, ion-assisted deposition reactive sputtering, and high-power impulse magnetron sputtering (HIPIMS) that produce higher energy flux of sputtered comparing with DC magnetron sputtering and ionized atoms are delivered to the growing surface in pulses repeated at certain frequency [5, 7]. Some materials deposited by magnetron sputtering have found applications in energy such as in gas turbine blade coating and solar panels, electronics/microelectronics application in flip-chip backside metallization and sensors, and many other applications in various fields.

1.2 History of boron carbon nitride (BCN) thin film technology

In the recent years, thin film technology was applied in the field of semiconductors science. More interestingly, BCN films represented a potential material as protective and hard coatings for cutting tools and for other wear-resistance uses [8–14]. Drude in 1889 discussed the earliest fabrication of thin films under vacuum with unique characteristics on the glass of discharge tubes [15]. The principal properties of the materials could be improved by the formation of thin films instead of other structural arrangements. For instance, few numbers of microns of gold material coated onto glass surface make the glass conductive. Furthermore, thin film technology was used to prepare metastable phases at low temperature especially with applying plasma techniques such as sputter deposition and plasma assisted chemical vapor deposition (PACVD) techniques. For example, cubic boron nitride could be prepared easily at lower pressure and temperature than bulk fabrication processes. Moreover, PACVD techniques were employed to prepare polycrystalline diamond at 20 mbar pressure and lower than 1000 K temperature [16]. Thin film technology has been applied to semiconductor and photovoltaic cell technologies [17, 18]. It is well known that elemental solids of group IVA and compounds between IIIA and VA groups were applied in the aforesaid technologies because of their excellent physical and electrical properties. Within the next sections, the unique behaviors of BN and B_4C materials will be discussed as well as the promising properties resulting from combining these materials to synthesize BCN thin films.

1.2.1 Boron nitride (BN) thin films

Diamond, c-BN, and boron carbide (B_4C) are among the hardest known materials apart from nanocomposites or nano-multilayer materials. The structures of diamond and c-BN are very close to each other. Graphite and h-BN exhibit layered structures with weak van der Waals forces. More interestingly, graphite is a semi-metal while h-BN is an insulator.

Boron nitride material is a dry lubricant with excellent properties, which can be altered with respect to the crystal morphology. BN layers were applied in electron-field emitters, high-temperature dielectrics, tribological devices, and optoelectronic systems [19–21]. BN material can be also used in solar cell industry as it can be implemented at high temperature [22–25]. It is noteworthy to mention that cubic boron nitride c-BN displays unique characteristics such as high thermal conductivity, wide band gap, extreme hardness, and negative electron affinity [26–34]. In addition, c-BN was used in a wide range of applications because of its novel chemical and physical behaviors. Chemical vapor deposition (CVD) and physical vapor deposition (PVD) can be utilized to provide a high-energy ion bombardment on the growing surface and this leads to accumulation of the compressive stress [35–39]. The compressive stress can be diminished by introducing 25% hydrogen into the reactive gasses [40–43]. By using CVD and sputter processes, c-BN films can be fabricated with a thickness more than 1 μm [44–46].

Many researchers paid their attention for the RF sputtering of BN sheets. One example of this, BN thin films were RF deposited on a glass substrate for gas sensor, optoelectronic, and beam-splitter applications [47]. High-pressure RF reactive magnetron sputtering was used to investigate the surface and optical performance. The results showed that the synthesized sheets offered good purity, homogeneity as well as low hydrophobicity. Furthermore, the c-BN phase can be produced by altering the Ar flow. The XRD analysis of the prepared films showed that the crystal structures are cubic and hexagonal. The crystal structures can be modified by changing the N_2:Ar ratio. In addition, high-quality c-BN thick films were deposited on Si substrates by Zhao et al. by introducing hydrogen gas into N_2/Ar mixture gasses. The incorporation of hydrogen gas decreased the deposition rate by suppressing the growth of h-BN. At a substrate temperature of 400 °C and bias voltage of − 80 V, a 4.5 μm-thick c-BN sheets with over 95% cubic concentration were produced [48].

1.2.2 Boron carbide (B_4C) thin films

Among many different non-metallic materials such as silicon, alumina or nitride boron carbide owned a great property which has a high melting point (> 2400 °C) [49], excellent mechanical properties [50], outstanding hardness [51], great resistance to chemical agents, low specific weight, and high neutron absorption cross-section [52, 53]. Boron carbide atomic structure has been widely discussed in the various literature [54–58]. Due to its superior properties, B_4C is used in several

applications for example in high-technology industries, lightweight body armors [59], abrasive wear-resistant materials, power generation in deep-space flight devices, and high-temperature thermoelectric conversion [60–67]. In addition, the crystal structure of boron carbide has been identified for a long time [68]. Boron carbide crystal structure contained 12-atom icosahedral clusters located at the vertices of a rhombohedral lattice and connected by direct covalent bonds [69]. The rhombohedral unit cell composed of 15 atoms corresponding to $B_{12}C_3$. The lattice fits the R3m space group, and there are three atoms of linear chains that join the icosahedra along the (111) rhombohedral axis, as shown in Fig. 1. Besides that, the structure can also be defined regarding a hexagonal lattice based on a non-primitive unit cell, and the close-packed plane of B_4C is the [0001] axis of the hexagonal lattice which corresponds to the [70] rhombohedral direction illustrated in Fig. 1 [71].

Studies of nuclear magnetic resonance (NMR) studied the crystal of stoichiometry close to $B_{12}C_3$ and found that the central position in the C–C–C chain was partially filled by boron (60%) [72]. By using IR absorption spectroscopy, it has confirmed the presence of the C–B–C chain in compounds such as B_4C [73]. Different techniques are used to prepare high-quality boron carbide; for instance, in an industrial area, it is made by using reduction of boron anhydrides, pressureless sintering, and hot pressing [74, 75]. Physical vapor deposition (PVD), pyrolysis of organics, and chemical vapor deposition (CVD) methods are used to synthesize B_4C in the laboratory [76–78]. However, CVD is divided into numerous methods that are used for depositing boron carbides such as plasma-enhanced chemical vapor deposition (PECVD) [79–82], synchrotron radiation-induced chemical vapor deposition (SRCVD) [83–85], classical-atmospheric or low-pressure chemical vapor deposition (c-CVD) [86–92], and hot filament (HFCVD) [93]. It is important to note that there are different conditions to control the deposition process like pressure, temperature, composition, and reactive gas mixture type [78]. The next section describes the structure and properties of BCN thin films prepared by combining B_4C and BN materials.

1.2.3 Boron carbon nitride (BCN) thin films

The Vickers hardness test on bulk cubic BC_2N (c-BC_2N) synthesized by Solozhenko et al. showed hardness of 76 GPa which is higher than that of a single crystal c-BN (62 GPa) [94]. This finding was motivated by Liu and Cohen calculations which showed that the bulk modulus (B) is directly proportional to the covalent character in bonding and inversely proportional to the bond length (d) in covalent materials [95]. The equation for tetrahedrally bonded covalent solids was expressed as following where λ is a measure of the ionicity of the compound: $B = \frac{19.71-2.20\lambda}{d^{3.5}}$

Therefore, hybrid compounds of IIIA-IVA-VA groups such as B–C–N ternary system represent a potential contestant for hard materials because of structural similarity between the three elements and their short bond distances. c-BC_2N prepared by Solozhenko is one instance of compounds containing B, C, and N, and demonstrating high Bulk Modulus value [94]. Liu et al. investigated the electrical behavior of layered BCN materials through pseudo-potential local-orbital calculations on hexagonal BC_2N (h-BC_2N). Liu et al. calculations were based on the mixture of these two similar structures and three different atomically arranged h-BC_2N single-layer atomic models. The obtained results confirmed that as the

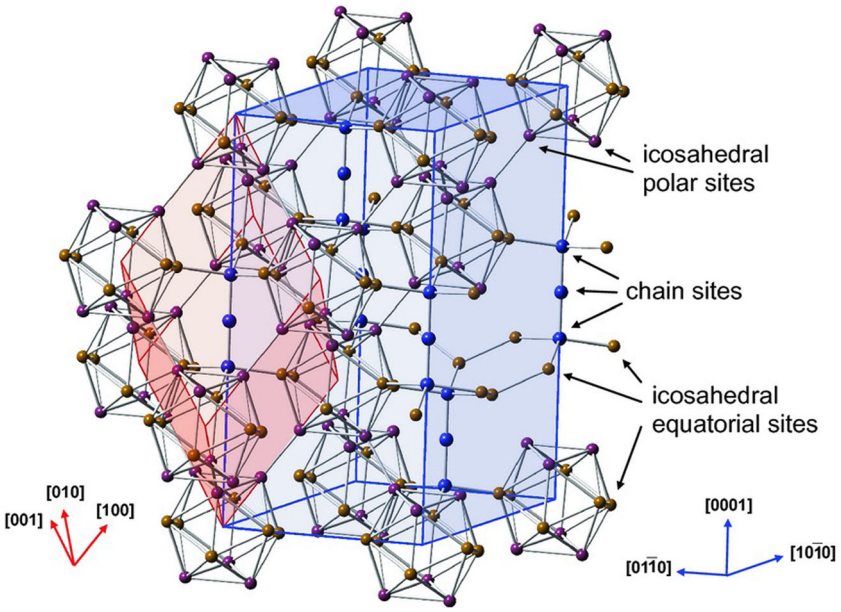

Fig. 1 Boron carbide lattice structure [69]

number of C–C and B–N bonds increases the total energy of B–C–N layers' decreases. In addition, these materials could be employed as adaptable semiconductors as they exhibit mutable band morphologies [96]. This behavior was attributed to that the atomic arrangements of the atoms can tune the electrical characteristics without altering the atomic compositions.

2 Processing parameters of BCN thin film synthesis by sputtering technique

The structure and composition of the deposited films can be controlled by numerous parameters. These parameters will be discussed in details in the next sections.

2.1 Gasses flow ratio

It is noteworthy to report that Lousa et al. presented the results of using reactive RF magnetron sputtering to deposit a thin film of BCN by applying B_4C target in a variable N_2/Ar atmosphere that show highly active nitrogen combination mechanism. The structure, film composition, and mechanical properties were studied and demonstrated that in the plasma gas, the variation of N_2/Ar mixture from 0 to 10% showed an increase of the N content in BCN films from 0 to 40% while the growth rate of the film increased around 0.5 mm/h. The film hardness decreased about 14 GPa and also the film stress reduced to 3 GPa. As a result, a suitable composition amount of N_2 and Ar gasses can be designated to achieve films with acceptable low stress though preserving a high hardness, which is needed in hard coating applications [97]. A preparation of BCN thin films also done by Yokomichi et al. using magnetron sputtering with two different targets which are BN pellets and graphite in the flow of a mixture of Ar and N_2 gas. They found that to enhance the senility of the sample, boron has to incorporate into BN networks. The concentration of B in films that produced during the flow of Ar gas was higher than in the films produced using N_2 gas, while the deposition rate was higher in the films with using N_2 gas compared to the film produced with Ar gas. The defect properties were investigated by using electron spin resonance (ESR) that found the linewidth improved because of the combination of B atoms which resulted from the hyperfine interaction between boron nucleus and carbon dangling bond electron [98]. From another hand, the effect of using Ar/N_2 gas ratio on BCN films and their microstructure has been reported by Nakao, S. and his co-authors by using RF magnetron sputtering with a flow of Ar/N_2 gasses [99]. Both of half-moon shaped B_4C as BC-side and graphite as G-side targets, while two of Si (100) substrates were used. Different techniques were applied such as electron FE-SEM/EDX, FT-IR, XPS, UV Raman measurements, and nanoindenter test to investigate the compositional, structural and the mechanical behaviors of the films. The results demonstrated that the quantity of C–N bonds enhanced when increasing N_2 ratio, whereas the concentration of B decreased even in G-side. Otherwise, the level of C increased.

Moreover, Todi et al. examined the optical behavior of the RF sputtered BCN films as a function of N_2/Ar gas ratio during the deposition process. The film composition and deposition speed were dependent on the mixture gas ratio. It was revealed that the transmittance was enhanced with the initial nitrogen introduction but did not alter with higher N_2/Ar gas ratios. The optical band gap of the deposited films was improved up to 0.75. The optical band gap ranged from 2.2 to 3.0 eV (Fig. 2) and this indicates the possible linear trend between that of BC (2.0 eV) and BN (4.0 eV). Therefore, this performance can be applied to bandgap engineered devices [100]. It is noteworthy to mention that Yue et al. used Ar/CH_4 gas mixture to deposit BCN thin sheets from BN targets [101]. It was revealed that the deposited films exhibited a structure of polycrystalline BC_2N. Moreover, at 10% CH_4 partial pressure, the deposited BCN film provided semiconductor characteristics with an activation energy of 0.8 eV.

2.2 N_2 flow rate

More interestingly, Tavsanoglu et al. investigated the mechanical, microstructural, tribological, and chemical behaviors of BCN films deposited onto silicon and steel substrates by using B_4C target with the flow of N_2 gas from 0 to 50%. The coat deposited with reactive DC magnetron sputtering and characterized by FE-SEM, electron probe microanalyzer (EPMA), XRD analyses, FTIR, and SIMS techniques. They studied the chemical composition, microstructures, chemical bonding structures, crystallinity, and mechanical and the tribological characteristics. The results showed a significantly reduced hardness, elastic modulus, and wear resistance and also

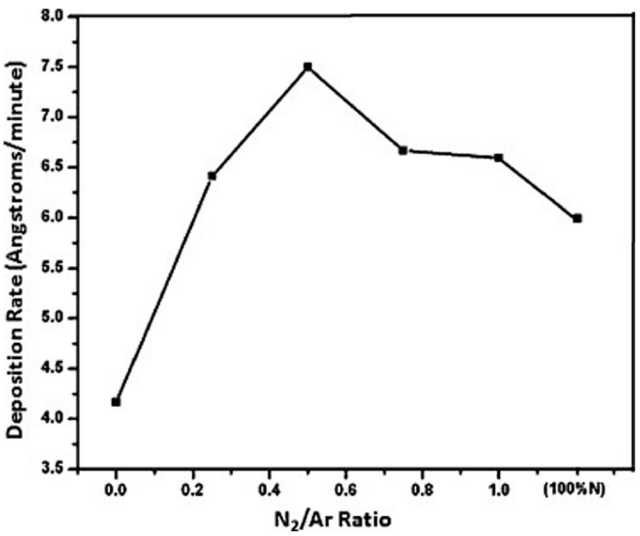

Fig. 2 Optical band gap of the deposited BCN films as a function of N_2/Ar gas ratio [100]

reduction in the concentration of boron and carbon in BCN films with the increase of flow of N_2 in the coating composition. It is worth mentioning that it can be facile to deposit the ternary triangle B–C–N with tailored behaviors by using reactive DC magnetron sputtering with altering N_2 flow rates [102].

2.3 Deposition temperature

For optical protection applications, a combination target of graphite and h-BN was employed to grow BCN thin films by RF magnetron sputtering on silicon and glass substrates at different temperatures ranged from 250 to 550 °C [103]. It was revealed that the elemental chemical binding states and composition of the deposited BCN films were significantly affected by the deposition temperature. Moreover, at higher temperatures, the films with a higher portion of sp^3 bindings of boron, carbon, and nitrogen were produced. The refractive index and optical bandgap were observed to be in the range of 2.1–2.4 and 1.48–2.00, respectively. It was observed that, as the deposition temperature increases, the refractive index decreases and the optical bandgap increases. The fabricated amorphous $B_{25}C_{40}N_{35}$ at 550 °C exhibited excellent optical behavior because of high fractions of sp^3 binding states. Tunable bond contents offer a significant parameter in controlling the physical characteristics of the materials.

2.4 Annealing

It is worth mentioning that Xu et al. studied the mechanical, structure, and scratch behavior of annealing temperature BCN thin films [13]. The films were prepared on Si substrate by using B_4C desk and graphite ring composite targets in a direct current (DC) unbalanced magnetron sputtering at a mixture of Ar/N_2 gasses. After that, the BCN films were annealed in the range of temperatures. They found that BCN film owns a great vacuum thermal stability even with high annealing temperature like 1000 °C, as well as the stability of the structure and amorphous phase of the film did not affected. Also, the results show that at the same temperature 1000 °C the films demonstrated an excellent interfacial adhesion. Furthermore, increasing the annealing temperatures leads to a decrease in the elastic modulus and hardness properties of the films. The BCN films exhibited the strongest scratch resistance behavior at 600 °C.

Another work investigated the impact of annealing temperature on the optical behaviors of BCN thin films. Todi et al. fabricated BCN thin films on Si wafers using RF magnetron sputtering with the B_4C target, and by varying Ar and N_2 gas flow ratio [104]. The study conducted various annealing temperatures in dry oxygen at a range of 300 to 700 °C. The results showed that the optical transmission property improved with N_2 incorporation within the deposition process and also at higher annealing temperatures. Besides that, annealing at higher temperatures led to decreasing the concentration of C and N in the film which confirmed that both C and N are very sensitive to temperature. The optical energy gaps measured from the absorption data also affected by annealing temperatures. XPS analysis showed that the chemical modifications correlated to the changes in optical properties of the films.

2.5 Sputtering power

The BCN thin films with hybridized B–C–N bonds were synthesized and sputtered on silicon wafers by Kim et al. using the RF magnetron sputtering of separate boron and carbon sources. The influence of the sputtering power of carbon target on the composition, morphology, and binding states of the fabricated films was reported [105]. B–N, B–C, C–N, and C–C chemical bonds were recognized in the deposited films. The FT-IR (Fig. 3) and XPS spectra exhibited the amorphous phase in most of BCN films. Increasing the sputtering power of carbon target induced strong B–C, C–C, and C–N bonds, which increased the elastic coefficients, hardness and elastic modulus of the synthesized films.

Liu, L. and co-authors explained the synthesis of BCN films by using RF magnetron sputtering on Si (100) substrate using dual targets containing h-BN and graphite in a mixture of Ar and N_2 gas [106]. The study investigated atomic-level of the films that composed of B, C, and N atoms. They explored the effect of the sputtering power at a range of 80 to 130 W on the composition of BCN films and their atomic fractions. It is worth mentioning that, at 110 W sputtering power, both B and N reache the highest of the atomic fractions while C atoms fraction reaches the minimum. Furthermore, the closest stoichiometry of BC_3N produced at two sputtering power conditions 80 W and 130 W. However, the closest sample to the stoichiometry of BC_2N found in the deposited range 100 and 120 W, and lastly, the closest sample to the composition of BCN found in the sample prepared at 110 W.

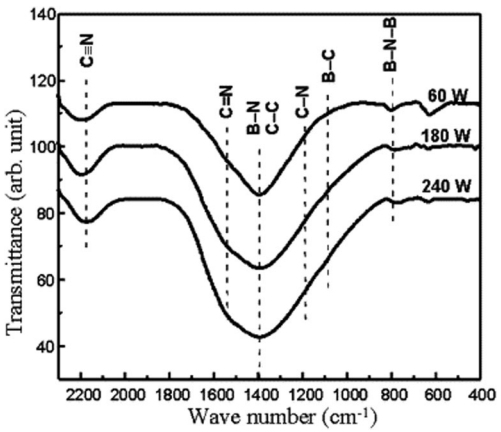

Fig. 3 FT-IR spectra of synthesized BCN films at various carbon sputtering power [105]

2.6 Bias voltage

The morphology of BCN thin films can be investigated by measuring the bond contents. For example, Zhuang et al. deposited BCN films using boron and carbon targets with controlling the substrate temperature and bias voltage [107]. The composition of the fabricated films was unresponsive to the bias voltage regardless of the substrate temperature (25 °C or 400 °C). By changing the bias voltage and substrate temperature, the bond contents in the deposited films can be controlled. At 400 °C, the sp^3-BN, sp^2-CC, sp^2-CN, and CN bonds content were increased while those of B–C and sp^2-BN were declined. Figure 4 demonstrates the cross-sectional SEM micrograph of a deposited thin film at 400 °C and bias voltage of − 75 V.

In addition, Liu et al. synthesized BCN thin films by using RF magnetron sputtering through using a combination targets containing h-BN and graphite on Si (100) substrates with a fix distance of 6.5 cm between the substrate and the target. A mixture of N_2 and Ar gasses flows into the chamber. They investigated the effect of P_{N2}/P_{N2+Ar}, substrate bias voltage on BCN composition films, and total pressure. The deposited films were successfully shown to be chemically bonded to B, C, and N elements altogether and atomic-level hybrids. Furthermore, decreasing the P_{N2}/P_{N2+Ar} to 0% results in reducing the contents of B, N and increasing the atomic fraction of C atoms. Similarly, in an optimum total pressure, at higher bias voltages, BCN films displayed minimal content of B and N and higher C content. Whereas, decreasing the total pressure and bias voltage led to the reduction of the content of C atoms to the minimum and increased the fractions of B and N atoms to the maximum [108].

3 Studies of sputtered BCN thin films

The physical and chemical behaviors of BCN films attracted a growing attention of researchers in the recent years. There are different studies conducted on BCN thin films deposited by using magnetron sputtering technique.

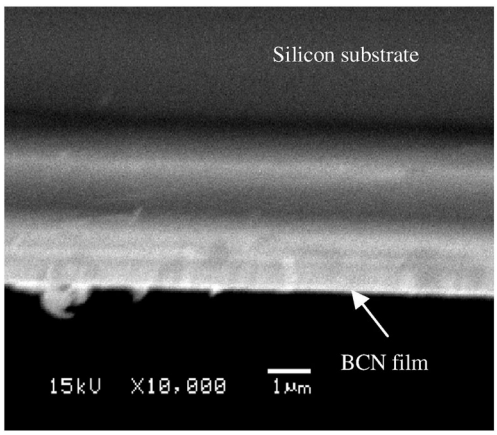

Fig. 4 Cross-sectional SEM micrograph of BCN thin film deposited at 400 °C and bias voltage of − 75 V [107]

3.1 Mechanical studies

For hardness investigations, Prakash et al. synthesized BCN thin films as potential low-k candidates for inter-dielectric sheets for ultra-large scale integrated (ULSI) circuits. The hardness and electrical properties of BCN thin films were also discussed. In their work, BCN thin films were prepared by radio frequency (RF) target sputtering from B_4C and dual target sputtering by using B_4C target (RF) and BN target (DC) with Ar and N_2 flow. The elastic modulus (E) and hardness (H) of the synthesized BCN films were studied as a function of different parameters. At certain power and N_2/Ar flow ratio, the hardness was declined and this performance can be designed to control the hardness for the desired application. More interestingly, as the N content and substrate temperature increase, the dielectric constant decreases. In addition, when the temperature was increased, the hardness of BCN films was clearly increased [109].

BCN films were also synthesized by DC and RF magnetron sputtering using a combination of B_4C, BN, and C targets in Ar/N_2 ambient to study the mechanical and dielectric properties such as mass density, hardness, Young's modulus, and dielectric constant [110]. They examined the chemical composition and chemical bonding of the deposited films using XPS and FTIR. It was found that all BCN films have relatively low mass densities varied from 2.0 to 2.5 g/cm^3. BCN films displayed high values of hardness ranging between 30 and 40 GPa and Young's modulus of ~ 285 GPa.

3.2 Etching studies

Prakash et al. investigated the wet chemical etching of BCN thin films deposited using dual magnetron sputtering of B_4C (DC) and BN (RF) targets in a mixture of N_2/Ar ambient using [111]. They used a combination of H_3PO_4, HNO_3, and CH_3COOH as a typical aluminum etchant to test its feasibility as a good etchant for BCN thin films. The etching studies were performed on BCN films that were deposited at room temperature, 200 °C and 300 °C, as a function of various N2/Ar gas flow ratios. It was found that the etching rate of BCN films decreases with increasing deposition temperature.

3.3 Optical studies

The optical behavior of BCN films was discussed by Prakash et al. BCN films were fabricated by RF magnetron sputtering of BN target and DC sputtering of the B_4C target in Ar and N_2 gas atmosphere. Different parameters such as N_2/Ar flow ratio, deposition pressure, and deposition temperature influenced the optical behavior of the deposited BCN films

effectively. Moreover, when the N_2 loading in the BCN film was increased, the optical transmission was increased significantly. The rise in substrate temperature affected the transmission slightly. The calculated optical band gap using Tauc plot was increased with increasing the N_2/Ar flow ratio [70].

3.4 Photoluminescence studies

Prakash et al. conducted a study about photoluminescence (PL) on BCN thin films. They used dual target sputtering utilizing B_4C (DC), BN (R_f) targets and a mixture of N_2 and Ar gas flow ratio with increasing the substrate deposition temperature to 200 °C and 400 °C. PL spectra of BCN films exhibited in the visible region two sharp peaks at 498 nm and 599 nm. The PL spectrum of the film deposited at 400 °C displayed the highest PL intensity. The increased PL intensity with increasing the deposition temperature was attributed to the improved crystalline quality of the BCN films. [112].

3.5 Copper diffusion studies

Copper is highly diffusing in oxide-based low-k films which causes significant precision problems. However, BCN is inactive and strong to use in diffuse of numerous interconnect metal ions, for instance, copper (Cu) even at higher annealing temperatures. Prakash A. and Sundaram K. reported the diffusion of copper in BCN thin films deposited by dual target sputtering using B4C (DC) and BN (RF) as targets. Secondary-ion-mass spectrometry (SIMS) analysis was performed to study the diffusion of Cu into BCN films while X-ray photoelectron spectrometry (XPS) was equipped to measure the elemental stoichiometry of the film. The outcomes illustrated that increasing the concentration of boron in the BCN thin film leads to the increase of the Cu diffusion whereas, annealing the film in the range of 200–400 C has minimal copper diffusion effects in the BCN films. [113].

3.6 Electrical studies

The successful deposition of BCN thin films by RF magnetron sputtering and DC sputtering of BN and B_4C targets, respectively in Ar and N_2 flow was also achieved to investigate the electrical characteristics of BCN films. Metal-insulator-metal (MIM) sandwich structure such as Al-BCN-Al was also prepared. It was noted that the electrical behavior of the synthesized BCN films can be efficiently controlled by N_2/Ar flow ratio, deposition pressure, and deposition temperature. Increasing the N_2 loading in the BCN films and substrate temperature reduced the dielectric constant of the produced BCN films. The breakdown voltage was increased with N_2. Furthermore, with increasing the substrate temperature, the breakdown voltage was increased initially then followed by a slight decrease. The resistivity of the deposited BCN films was noticed to be constant and can be slightly changed by increasing the substrate temperature [114].

3.7 XPS studies

Dual magnetron sputtering was used by Prakash et al. to optimize the processing parameters of BCN thin film synthesis. The deposition process was optimized by target power levels, N_2/Ar flow ratio, and substrate temperature. In this approach, B_4C and BN targets were co-sputtered with nitrogen gas to deposit the BCN films. It was realized that keeping DC power to B_4C target constant while increasing RF power to BN target increased the deposition rate. In contrast, keeping RF power to BN target constant while increasing DC power to B_4C target did not change the deposition rate. The deposition rate was declined at N_2/Ar gas ratio of 0.25 to 0.75 and 20 W DC while no clear behavior was noticed at 40 W DC. In addition, the deposition rate was declined and tended to increase at 400 °C. A clear BCN phase formation for the BCN films fabricated at both 20 W and 40 W DC and different N_2/Ar flow ratios and temperatures was revealed from XPS spectra. It was noteworthy to mention that clearer BCN peaks were noticed for 40 W DC deposition compared to 20 W DC deposition. Furthermore, the BCN films deposited at 20 W DC exhibited a constant N1s peak (BN peak) with increasing the N_2/Ar flow ratio while N1s peak was shifted towards higher binding energies at 40 W DC deposition, indicating a higher content in carbon. Higher loading of sp^2-NC bonds was noticed. C1s peak (B–C peak) intensity was decreased for films deposited at 20 W DC and remained constant for films synthesized at 40 W DC. For films deposited at 20 W DC, the broadening of C-N peak was observed at higher N_2/Ar flow ratio and becomes prominent at N_2/Ar flow ratio of 1. The C content was declined and revealed by the slight shift of C–N peak towards lower binding energy at higher flow ratios. For 20 W DC deposition, BCN peak was increased while BN peak remained constant whereas, for 40 W DC deposition, BCN peak broadens with increasing N_2/Ar flow ratio and becomes prominent at N_2/Ar gas ratio of 1 [115]. To investigate the physical and the chemical characteristics of deposited films, graphite, and B_4C targets were applied in RF sputtering by Essafti et al. to deposit amorphous CN, amorphous BC, and amorphous BCN thin films on silicon substrates. It was found that carbon atoms bound to nitrogen atoms majorly as sp^2 C=N rather than sp^3 C–N and exist as C–C bonds in the deposited BCN films. In addition, C=N and B–N bonds were also formed. The films were deposited with varying proportions and diverse bonding forms. The great variation in the shape and the binding energies of the C1s core level XPS

spectra indicated the difference in the morphology of the synthesized films [116].

3.8 Corrosion studies

Composites are applied in a wide range of applications because of their promising properties [117–125]. To illustrate, the corrosion behavior of BCN films has been attracted a growing attention of researchers to allow their application in different environments. The electrochemical polarization and dissolution rate of a deposited BCN thin film in acidic, neutral, and alkaline mediums were studied by Byon et al. The dissolution rate of $B_{1.0}C_{2.4}N_{1.0}$ thin film was declined in NaOH < NaCl < HCl solutions (Fig. 5a). In 1 M NaOH medium, it was revealed that as the C ratio increases as the dissolution rate of the BCN film decreases (Fig. 5b). In addition, a $B_{1.0}C_{(3.2–4.4)}N_{1.2}$ thin film was noticed to exhibit a superior corrosion-resistant performance [126].

3.9 Raman spectroscopy studies

Raman spectroscopy is a technique applied to measure the wavelength and intensities of inelastically scattered light by measuring the change in rotational, electronic or vibrational energy of a molecule. The properties and microstructures of the films can be investigated by Raman spectroscopy [127]. The long-range ordered crystalline structure can be predicted from Raman results. To illustrate, Tsai et al. used pulsed-DC magnetron sputtering technique to deposit BCN films using B_4C target under Ar/N_2 gas flow. Numerous processing factors were discovered to grow BCN films with high c-BN content [128]. To characterize the composition and phases, Raman spectroscopy with other techniques was used. By changing temperature and substrate bias, the deposited BCN films displayed h-BN, c-BN, wurtzite-BN (w-BN) phases and their mixed phases. By controlling the substrate bias and stage deposition technique, 90% c-BN film was obtained with clear facets and grains [128].

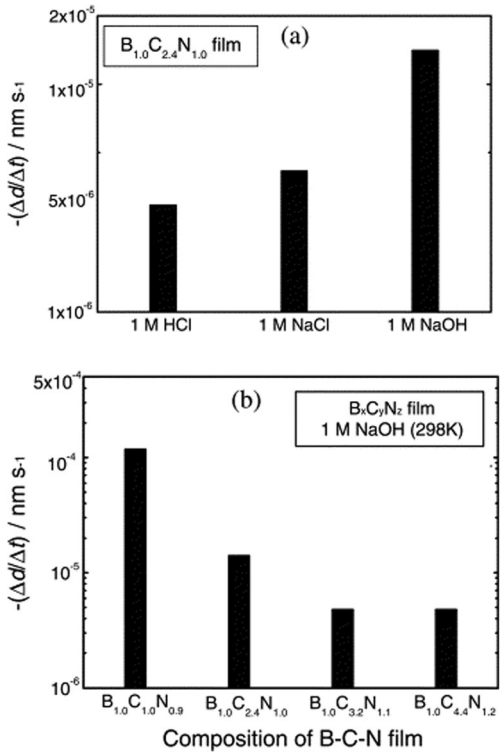

Fig. 5 Dissolution rate ($-\Delta d/\Delta t$) of **a** $B_{1.0}C_{2.4}N_{1.0}$ films in 1 M HCl, 1 M NaCl, and 1 M NaOH mediums, **b** $B_{1.0}C_{(0.5–4.4)}N_{(0.9–1.2)}$ films in 1 M NaOH medium [126]

4 Metal-insulator-metal (MIM) devices based on BCN thin films

Prakash A. and Sundaram K. synthesized BCN thin films by RF magnetron sputtering using B_4C target at various flow ratios of N_2 and Ar gasses and deposition temperatures to study the electrical properties of metal-insulator-metal (MIM) devices. They found that increasing the N_2 gas in the BCN film and the substrate temperatures leads to drop the dielectric constant but increasing the dielectric breakdown strength and the resistivity. Moreover, the highest dielectric breakdown strength of 3.4 MV/cm of BCN films achieved with a dielectric constant of 2.13 and resistivity of 3×10^{12} Ω.cm [129]. Another paper conducted by Prakash et al. for MIM devices tested for their potential UV photodetection capability by using BCN films applied in harsh environment applications. They used dual target RF magnetron sputtering, BN target as DC sputtering and B_4C as RF magnetron sputtering with N_2 and Ar as processing gas to form BCN films. Glass substrate used to produce MIM structure, deposited by aluminum strips as a bottom electrode using a mechanical mask in a thermal evaporation technique and loaded in the sputtering system to deposit a thin film of BCN of a thickness of 100 to 120 nm. The last step ended by creating the top electrode through depositing a number of gold strips over the BCN film, a thin layer of gold fabricated by using thermal evaporation process to form a transparent top electrode for the photo-detector window. Using UV photocurrent measurements, the optoelectronic performance of the BCN MIM device was examined using UV photocurrent measurements. The device achieved a UV photocurrent response of two orders higher with respect to dark current in the range − 3 to 3 V [130].

Table 1 represents different processing parameters used to prepare thin BCN films. This table summarizes the targets used in both of RF and DC powers, deposition gasses, and the various temperatures used during the deposition and the main results.

Table 1 Summary for different processing parameters used to prepare BCN thin films

Targets	Authors	Characterization techniques	Flow rate of gas	Temperature	Power	Results
BCN, B_4C target	Lousa et al. [97]	Dektak 3030 surface profiler, XPS, SIMS, FT, IR and Raman spectroscopies and the dynamical microindentation	N_2/Ar is diverse from 0 to 10%	500 °C	300 W of Rf	•Hardness decreased about 14 GPa and also the film stress reduced to 3 GPa.
BCN, BN pellets and graphite targets	Yokomichi et al. [98]	XPS, infrared absorption (IR) and XRD	Ar and N_2	30 °C, 100 °C, or 200 °C.	100 W of Rf	•Enhance the senility of the sample by incorporating the boron into BN networks. •Linewidth improved because of the combination of B atoms
B_4C and graphite targets	Nakao, S. and his co-authors [99]	Electron FE-SEM/EDX, FT-IR, XPS, UV Raman measurements and nanoindenter test	Ar/N_2	RT	200 W of Rf	•The quantity of C–N bonds enhanced when increasing N_2 ratio, whereas the concentration of B decreased even in G-side. Otherwise, the level of C increased.
B_4C	Todi et al. [100]	XPS and SIMS analysis	N_2/Ar gas ratio	100 °C	200 W of DC	•Transmittance was enhanced with the initial nitrogen introduction but did not alter with higher N_2/Ar gas ratios. •The optical band gap of the deposited films was improved up to 0.75.
BN targets	Yue et al. [101]	XPS, XRD, and FTIR	Ar/CH_4 gas mixture	450 °C	–	•At 10% CH_4 partial pressure, the deposited BCN film provided semiconductor characteristics with an activation energy of 0.8 eV.
B_4C target	Tavsanoglu et al. [102]	FE-SEM, electron probe microanalyser (EPMA), XRD analyses, FTIR and SIMS techniques	Ar/N_2 gasses	250 °C	500 W	•Significantly decreased of the hardness, elastic modulus, and wear resistance and also decreased in the concentration of boron and carbon in BCN films with the increase of flow of N_2 in the coating composition.
h-BN and graphite	Lei M., et al. [103]	Ellipsometer, XPS, and TEM	Ar/N_2 gasses	Ranged from 250 to 550 °C	60 W of Rf	•The refractive index and optical bandgap were observed to be in the range of 2.1–2.4 and 1.48–2.00, respectively. •The fabricated amorphous $B_{25}C_{40}N_{35}$ at 550 °C exhibited excellent optical behavior because of high fractions of sp^3 binding states
B_4C and graphite ring	Xu et al. [13]	XPS, FTIR, XRD, and CSM	Ar/N_2 gasses	450 °C	210 W	•The film owned a great vacuum thermal stability even with high annealing temperature like 1000 °C, as well as the stability of the structure and amorphous phase of the film did not affect.
B_4C target	Todi et al. [104]	Optical energy and XPS	Ar/N_2 gas flow ratio	300 to 700 °C	200 W of DC	•The optical transmission property improved with N_2 incorporation within the deposition process and also at the higher annealing temperature. •XPS analysis was proved that the chemical modifications were correlated to the changes in optical properties of the films.

Table 1 (continued)

Targets	Authors	Characterization techniques	Flow rate of gas	Temperature	Power	Results
Carbon target	Kim et al. [105]	FT-IR, HRTEM, and XPS spectra	Ar/N_2 gas flow ratio	RT	150 W of Rf and 60–240 W of DC	•Increasing the sputtering power of carbon target induced strong B–C, C–C, and C–N bonds which increased the elastic coefficients, hardness and elastic modulus of the synthesized films.
h-BN and graphite	Liu, L., and co-authors [106]	XPS, FTIR, and XRD	Ar/N_2 gas flow ratio	400 °C	80 W to 130 W	•At 110 W, both B and N reach the highest of the atomic fractions while C atoms fraction reaches the minimum. •The closest stoichiometry of BC_3N produced at two sputtering power conditions which are 80 W and 130 W.
Boron and carbon targets	Zhuang et al. [107]	SEM, XRD, FTIR, and XPS	Ar and N_2 flow	25 °C and 400 °C	100 W of Rf	•At 400 °C, the sp^3-BN, sp^2-CC, sp^2-CN, and CN bonds content were increased while those of B–C and sp^2-BN were declined
h-BN and graphite	Liu et al. [108]	XRD, FTIR, and XPS	Ar and N_2 flow	400 °C	110 W of Rf	•The deposition films were successfully shown a chemically bonded to B, C and N elements altogether and atomic-level hybrids. •Decreasing the P_{N2}/P_{N2+Ar} to 0% result of reducing the contents of B, N and increasing the atomic fraction of C atoms.
B_4C and BN target	Prakash et al. [109]	Nanoindentation Experiments and FTIR	Ar and N_2 flow	200 °C, 300 °C 400 °C and 500 °C	DC and RF power of 200 W and 150 W	•The elastic modulus (E) and hardness (H) of the synthesized BCN films were studied as a function of different parameters. •At certain power and N_2/Ar flow ratio, the hardness was declined and this performance can be designed to control the hardness for the desired application.
B_4C, BN, and C targets	Prakash A, Todi V, Sundaram KB, et al. [110]	XRD, XPS, and FTIR	Ar/N_2 ambient	–	DC or RF power was increased from 100 to 200 W with the other kept constant at 100 W.	•All films of BCN have relatively low mass densities alternating from 2.0 to 2.5 g/cm^3. •In pure Ar gas, either (C/BN) or (B_4C/BN) targets BCN films displayed high values of hardness ranging from 30 to 40 GPa and Young's modulus ~ 285 GPa.
B_4C and BN	Prakash A, Sundaram KB [111]	XPS	Ar and N_2 gas	RT, 200 °C and 300 °C	250 W of Rf and 20 W of DC	•The H_3PO_4, HNO_3, and CH_3COOH as a typical aluminum etchant to test its feasibility for BCN thin films while the highest temperature dependent reaction and calculated activation energy were at 200 °C and 0.9 eV respectively.
BN and B_4C target	Prakash et al. [70]	UV-Visible spectrophotometer	Ar and N_2 gas	RT, 200 °C, 300 °C 400 °C and 500 °C	250 W of Rf and 20 W of DC	•As the N_2 loading in the BCN film was increased, the optical transmission was increased significantly. •The rise in substrate temperature affected the transmission slightly.

Table 1 (continued)

Targets	Authors	Characterization techniques	Flow rate of gas	Temperature	Power	Results
						•The calculated optical band gap using Tauc plot was increased with increasing the N_2/Ar flow ratio.
BN and B_4C target	Prakash et al. [112]	XRD, FTIR, MCT	N_2/Ar gas flow ratio	RT, 200 °C, and 400 °C	–	•Two sharp PL peaks at 498 nm and 599 nm are found. •The deposition film at 400 °C displayed the highest PL intensity and the mentioned reason related to the high surface to volumes ratio and larger crystallite with fewer defects.
BN and B_4C target	Prakash, A. and Sundaram, K. [113]	SIMS, XPS	N_2/Ar gas flow ratio	200–400 °C	250 W of Rf and 20 W of DC	•Increasing the concentration of boron of BCN thin film lead to increasing the Cu diffusion whereas, the change of annealing temperature performed very small Cu diffusion influences in the BCN films
BN and B_4C target	Prakash et al. [114]	HP 4145B semiconductor parameter analyzer	N_2/Ar gas flow ratio	RT, 200 °C, 300 °C, 400 °C and 500 °C	200 W of Rf	•Metal-insulator-metal (MIM) sandwich structure such as Al-BCN-Al was also prepared. •Increasing the N_2 loading in the BCN films and substrate temperature reduced the dielectric constant of the produced BCN films.
BN and B_4C target	Prakash et al. [115]	XPS	N_2/Ar gas ratio of 0.25 to 0.75	200 °C and 300 °C.	20–40 W DC	•Clearer BCN peaks were noticed for 40 W DC deposition. •The BCN films deposited at 20 W DC exhibit a constant N1 s peak (BN peak) with increasing the N_2/Ar flow ratio while N1 s peak was shifted towards higher binding energies at 40 W DC deposition.
Graphite, and B_4C targets	Essafti et al. [116]					•Carbon atoms bound to nitrogen atoms majorly as sp^2 C=N rather than sp^3 C–N and exist as C–C bonds in the deposited BCN films. •The great variation in the shape and the binding energies of the C 1s core level XPS spectra indicated the difference in the morphology of the synthesized films.
99.9%-grade boron and 99.99%-grade carbon targets	Byon et al. [126]	Ellipsometer	N_2	–	180 and 150 W of r.f.	•The dissolution rate of $B_{1.0}C_{2.4}N_{1.0}$ thin film was declined in NaOH<NaCl<HCl solutions. •a $B_{1.0}C_{(3.2–4.4)}N_{1.2}$ thin film was noticed to exhibit a superior corrosion-resistant performance.
B_4C target	Tsai, T. et al. [128]	FTIR, SEM, TEM, AES, and Raman spectroscopy	N_2/Ar gas ratio	RT, 200 °C, 300 °C, 400 °C and 500 °C	200 W, and a 13.56 MHz RF	•The deposited BCN films displayed h-BN, c-BN, wurtzite-BN (w-BN) phases and their mixed •phases after changing temperature and substrate bias.

Table 1 (continued)

Targets	Authors	Characterization techniques	Flow rate of gas	Temperature	Power	Results
						•By controlling the substrate bias and stage deposition technique, 90% c-BN film was obtained with clear facets and grains.
BN and B_4C target	Prakash, A. and Sundaram, K. [129]	XPS	N_2/Ar gas ratio	RT, 200 °C, 300 °C, 400 °C and 500 °C.	200 W for Rf and DC	•Study the electrical properties of metal-insulator-metal (MIM) devices. •Increasing the N_2 gas in the BCN film and the substrate temperatures lead to drop the dielectric constant but increasing the dielectric breakdown strength and the resistivity.
BN and B_4C target	Prakash et al. [130]	XPS and UV illumination	N_2 and Ar	200 °C	250 W of Rf and 20 W of DC	•The optoelectronic performance of the BCN MIM device fabricated was examined and it was found that the device achieved a great UV photocurrent response of two orders of high extent on a dark current and variety from − 3 to 3 V with high photoresponsivity of 6 mA/W.

BCN boron carbon nitride, *BN* boron nitride, *XPS* X-ray photoelectron spectroscopy, *SIMS* secondary ion mass spectroscopy, *FT* Fourier transform, *IR* infrared absorption, *XRD* X-ray diffraction

5 Conclusion

Sputtering technique is considered as an excellent method to synthesize thin films with availability to use various types of substrates and deposit uniform films over a relatively large area. Many studies conducted the synthesis of BCN by RF magnetron sputtering and investigated different properties of the films and the effect of varying deposition parameters. The increase of N_2 flow resulted in a significant decrease in the elastic modulus, hardness, and wear resistance and led to reducing the amount of boron and carbon in BCN films. From the other hand, varying the temperature and annealing affected the refractive index and the optical bandgap. Furthermore, even at high annealing temperature at 1000 °C, it has been found that BCN films possess an unlimited vacuum thermal stability. Sputtering power also played a primary role in enhancing the elastic coefficients, hardness and elastic modulus of the synthesized films. Changing the bias voltage and substrate temperature allowed to control the bond contents in the deposited films. The hardness of BCN films can be improved by increasing the substrate temperature. The incorporation of about 20% of N_2 leads to producing BCN films with either electrically insulating behavior with a low dielectric constant or high mechanical characteristics. When the nitrogen content in the BCN film was surged, the optical transmission was increased dramatically while increasing the substrate temperature modified the transmission slightly. Furthermore, deposition BCN films at 400 °C offered the highest PL intensity, reducing the deposition temperature reduced the PL intensity. Cu diffusion could be increased by increasing the boron loading of BCN thin films whereas, changing the annealing temperature revealed very small Cu diffusion enhancement. Increasing the N_2 content and substrate temperature diminished the dielectric constant of the deposited BCN films. In addition, increasing the substrate temperature increased the breakdown voltage initially then followed by a slight decrease. The resistivity was found to be constant and can be slightly modified with increasing the substrate temperature. Corrosion studies revealed that $B_{1.0}C_{(3.2–4.4)}N_{1.2}$ thin films provided superior corrosion-resistant properties. BCN MIM devices achieved a UV photocurrent response of two orders higher with respect to dark current in the range − 3 to 3 V.

Funding information Dr. Talal M. Altahtamouni gratefully acknowledges Qatar University for funding the project: GCC Co-Fund Program Grant GCC-2017-007.

Compliance with ethical standards

Conflict of interest The authors declare that they have no conflict of interest.

References

1. Prakash A. Deposition and characterization studies of boron carbon nitride (BCN) thin films prepared by dual target sputtering (PhD Thesis) 2016
2. D.R. Gibson, I. Brinkley, E. Waddell, J.M. Walls, Proc. SPIE **7101**, 710108 (2008)
3. E. Pascual, E. Martı, J. Esteve, A. Lousa, Boron carbide thin films deposited by tuned-substrate RF magnetron sputtering. Diam. Relat. Mater. **8**, 402–405 (1999)
4. K. Koski, J. Ho, Voltage controlled reactive sputtering process for aluminium oxide thin films. Thin Solid Films **326**, 189–193 (1998)
5. A. Kossoy, R.L. Magnusson, T.K. Tryggvason, K. Leosson, S. Olafsson, Method to control deposition rate instabilities—high power impulse magnetron sputtering deposition of TiO2. J. Vac. Sci. Technol. A Vac. Surf. Film **33**, 21514 (2015)
6. T. Lohner, M. Serényi, D.K. Basa, N.Q. Khánh, Á. Nemcsics, P. Petrik, et al., Acta Polytech. Hungarica **5**, 23 (2008)
7. D. Depla, S. Mahieu, J. Greene, Handb. Depos. Technol. Film coatings **281**, 253 (1991)
8. P.D. Cuong, H.-S. Ahn, E.-S. Yoon, K.-H. Shin, Effects of relative humidity on tribological properties of boron carbide coating against steel. Surf. Coatings Technol. **201**, 4230–4235 (2006)
9. X. Deng, H. Kousaka, T. Tokoroyama, N. Umehara, Deposition and tribological behaviors of ternary BCN coatings at elevated temperatures. Surf. Coatings Technol. **259**, 2–6 (2014)
10. T. Hirte, R. Feuerfeil, V. Perez-Solorzano, T.A. Wagner, M. Scherge, Influence of composition on the wear properties of boron carbonitride (BCN) coatings deposited by high power impulse magnetron sputtering. Surf. Coatings Technol. **284**, 94–100 (2015)
11. Y. Li, X. Jia, W. Shi, S. Leng, H.A. Ma, S. Sun, F. Wang, N. Chen, Y. Long, The preparation of new "BCN" diamond under higher pressure and higher temperature. Int. J. Refract. Met. Hard Mater. **43**, 147–149 (2014)
12. V.S. Sulyaeva, Y.M. Rumyantsev, V.G. Kesler, M.L. Kosinova, Synthesis and optical properties of BCxNy films deposited from N-triethylborazine and hydrogen mixture. Thin Solid Films **581**, 59–64 (2015)
13. S. Xu, X. Ma, H. Wen, G. Tang, C. Li, Effect of annealing on the mechanical and scratch properties of BCN films obtained by magnetron sputtering deposition. Appl. Surf. Sci. **313**, 823–827 (2014)
14. F. Zhou, Q. Wang, B. Yue, X. Wu, L. Zhuge, X. Cheng, Mechanical properties and bonding structure of boron carbon nitride films synthesized by dual ion beam sputtering. Mater. Chem. Phys. **138**, 215–224 (2013)
15. Drude P Ueber Oberflächenschichten. II. Theil, Ann. Phys. **272**, 532 (1889)
16. R.N. Tiwari, J.N. Tiwari, L. Chang, M. Yoshimura, Enhanced nucleation and growth of diamond film on Si by CVD using a chemical precursor. J. Phys. Chem. C **115**, 16063–16073 (2011)
17. O. Sneh, R.B. Clark-Phelps, A.R. Londergan, J. Winkler, T.E. Seidel, Thin film atomic layer deposition equipment for semiconductor processing. Thin Solid Films **402**, 248–261 (2002)
18. A. Shah, P. Torres, R. Tscharner, N. Wyrsch, H. Keppner, Photovoltaic Technology: The Case for Thin-Film Solar Cells. Science **285**, 692–698 (1999)
19. X. Yang, H. Li, Y. Li, X. Lv, G. Zou, Synthesis and optical properties of purified translucent, orthorhombic boron nitride films. J. Cryst. Growth **312**, 3434–3437 (2010)
20. X. Yang, H. Li, Y. Li, X. Lü, S. Gao, P. Zhu, Q. Zhang, T. Zhang, G. Zou, Dependence of RF power on the phase transformation for boron nitride films deposited on graphite at room temperature. J. Cryst. Growth **311**, 3716–3720 (2009)
21. D. Jin-Xiang, Z. Xiao-Kang, Y. Qian, W. Xu-Yang, C. Guang-Hua, H. De-Yan, Chinese Phys. B **18**, 4013 (2009)
22. E. Weißmantel, T. Pfeifer, F. Richter, Electron microscopic analysis of cubic boron nitride films deposited on fused silica. Thin Solid Films **408**, 1–5 (2002)
23. Y. Panayiotatos, P. Patsalas, C. Charitidis, S. Logothetidis, Surf. Coatings Technol. **151–152**, 155 (2002)
24. X.W. Zhang, Y.J. Zou, B. Wang, X.M. Song, H. Yan, G.H. Chen, S.P. Wong, J. Mater. Sci. **36**, 1957–1961 (2001)
25. V. Dimitrov, S. Sakka, Electronic oxide polarizability and optical basicity of simple oxides. I. J. Appl. Phys. **79**, 1736–1740 (1996)
26. K. Teii, S. Matsumoto, Impact of low-energy ions on plasma deposition of cubic boron nitride. Thin Solid Films **576**, 50–54 (2015)
27. A. Schiitze, K. Bewilogua, H. Ltithje, S. Kouptsidis, S. Jager, Surf. Coat. Technol. **75**, 717 (1995)
28. A. Werbowy, J. Szmidt, A. Sokołowska, S. Mitura, RF plasma selective etching of boron nitride films. Diam. Relat. Mater. **9**, 609–613 (2000)
29. I. Bello, C.Y. Chan, W.J. Zhang, Y.M. Chong, K.M. Leung, S.T. Lee, Y. Lifshitz, Deposition of thick cubic boron nitride films: the route to practical applications. Diam. Relat. Mater. **14**, 1154–1162 (2005)
30. K. Bewilogua, M. Keunecke, K. Weigel, E. Wiemann, Thin Solid Films **469–470**, 86 (2004)
31. H. Yang, C. Iwamoto, T. Yoshida, Thin Solid Films **407**, 67 (2002)
32. B. Mårlid, K. Larsson, H. Carlsson J-O, Hydrogen and Fluorine Adsorption on the h-BN (001) Plane. J. Phys. Chem. B **103**, 7637–7642 (1999)
33. B. Wang, Y. Qin, F. Jin, J.F. Yang, K. Ishizaki, Pulse electric current sintering of cubic boron nitride/tungsten carbide–cobalt (cBN/WC–Co) composites: effect of cBN particle size and volume fraction on their microstructure and properties. Mater. Sci. Eng. A **607**, 490–497 (2014)
34. M.-E. Wang, G.-J. Ma, Dong C and Gong S-L 2014. Chinese Phys. B **23**, 66805 (2014)
35. F. Xu, M.F. Yuen, B. He, C.D. Wang, X.R. Zhao, X.L. Tang, D.W. Zuo, W.J. Zhang, Microstructure and tribological properties of cubic boron nitride films on Si 3 N 4 inserts via boron-doped diamond buffer layers. Diam. Relat. Mater. **49**, 9–13 (2014)
36. H. Yang, A. Chen, F. Qiu, Cubic boron nitride film residual compressive stress relaxation by post annealing. Diam. Relat. Mater. **20**, 1179–1182 (2011)
37. K.P. Loh, M. Nishitani-Gamo, I. Sakaguchi, T. Taniguchi, A.T. Diam, Relat. Mater., 8 (1296)
38. B. Mårlid, K. Larsson, J.-O. Carlsson, Nucleation ofc−BNon hexagonal boron nitride. Phys. Rev. B **64**, 184107 (2001)
39. H.S. Yang, J.Y. Zhang, A.M. Nie, X.B. Zhang, Chinese Phys. B **17**, 3453 (2008)
40. H.S. Kim, J.K. Park, W.S. Lee, Y.J. Baik, Variation of residual stress in cubic boron nitride film caused by hydrogen addition during unbalanced magnetron sputtering. Thin Solid Films **519**, 7871–7874 (2011)
41. J.-S. Ko, J.-K. Park, W.-S. Lee, Y.-J. Baik, The parameter space of hydrogen content added to Ar–nitrogen sputtering gas and substrate bias voltage for the formation of cubic boron nitride thin film

deposited by unbalanced magnetron sputtering method. Surf. Coatings Technol. **223**, 75–78 (2013)
42. I. Konyashin, V. Khvostov, V. Babaev, M. Guseva, J. Bill, F. Aldinger, The influence of excited hydrogen species on the surface state of sp2-hybridized boron nitride. Diam. Relat. Mater. **8**, 2053–2058 (1999)
43. J.K. Park, J.H. Lee, W.S. Lee, Y.J. Baik, Effect of substrate bias and hydrogen addition on the residual stress of BCN film with hexagonal structure prepared by sputtering of a B4C target with Ar/N2 reactive gas. Thin Solid Films **549**, 276–280 (2013)
44. S. Weidner, S. Geburt, S. Milz, J. Ye, S. Ulrich, C. Ronning, Extension of the cubic boron nitride thin film growth phase diagram. Diam. Relat. Mater. **22**, 88–91 (2012)
45. H.-G. Boyen, P. Widmayer, D. Schwertberger, N. Deyneka, P. Ziemann, Appl. Phys. Lett. **76**, 709 (2000)
46. M. Keunecke, E. Wiemann, K. Weigel, S.T. Park, K. Bewilogua, Thick c-BN coatings – preparation, properties and application tests. Thin Solid Films **515**, 967–972 (2006)
47. S. Pat, Anadolu Univ. J. Sci. Technol. Appl. Sci. Eng. **17**, 191 (2016)
48. Zhao Y, Gao W, Xu B, Li Y-A, Li H-D, Gu G-R *et al* 2016. Chinese Phys. *B* 25 106801
49. S. Tuff, J. Dubois, G. Fantozzi, G. Barbier, Densification, microstructure and mechanical properties of TiB2-B4C based composites. Int. J. Refract. Met. Hard Mater. **14**, 305–310 (1996)
50. I. Topcu, H.O. Gulsoy, N. Kadioglu, A.N. Gulluoglu, Processing and mechanical properties of B4C reinforced Al matrix composites. J. Alloys Compd. **482**, 516–521 (2009)
51. K.A. Schwetz, L.S. Sigl, L. Pfau, Mechanical properties of injection molded B4C–C ceramics. J. Solid State Chem. **133**, 68–76 (1997)
52. F. Thévenot, Boron carbide—a comprehensive review. J. Eur. Ceram. Soc. **6**, 205–225 (1990)
53. G. Bonnet, V. Rohr, X. Chen, J. Bernier, R. Chiocca, H. Issard, Pack. Transp. Stor. Secur. Radio. Mater. **20**, 98 (2013)
54. N. Vast, J. Sjakste, E. Betranhandy, Boron carbides from first principles. J. Phys. Conf. Ser. **176**, 12002 (2009)
55. K. Shirai, Electronic structures and mechanical properties of boron and boron-rich crystals (Part I). J. Superhard. Mater. **32**, 205–225 (2010)
56. K. Shirai, Prediction of phase diagrams for hard materials: application to boron crystals. Int. J. Thermophys. **35**, 1888–1899 (2014)
57. A.K. Suri, C. Subramanian, J.K. Sonber, T.S.R.C. Murthy, Synthesis and consolidation of boron carbide: a review. Int. Mater. Rev. **55**, 4–40 (2010)
58. H. Werheit, V. Filipov, U. Kuhlmann, U. Schwarz, M. Armbrüster, A. Leithe-Jasper, T. Tanaka, I. Higashi, T. Lundström, V.N. Gurin, M.M. Korsukova, Raman effect in icosahedral boron-rich solids. Sci. Technol. Adv. Mater. **11**, 23001 (2010)
59. X. Tao, L. Dong, X. Wang, W. Zhang, B.J. Nelson, X. Li, B4C-nanowires/carbon-microfiber hybrid structures and composites from cotton T-shirts. Adv. Mater. **22**, 2055–2059 (2010)
60. M.J. Zhou, S.F. Wong, C.W. Ong, Q. Li, Microstructure and mechanical properties of B4C films deposited by ion beam sputtering. Thin Solid Films **516**, 336–339 (2007)
61. M. Chen, J.J.W. McCauley, K.J.K. Hemker, Science **99**, 1563 (2003)
62. S.P. Dodd, G.A. Saunders, B. James, J. Mater. Sci. **37**, 2731–2736 (2002)
63. R. Ma, Y. Bando, Investigation on the growth of boron carbide nanowires. Chem. Mater. **14**, 4403–4407 (2002)
64. W.Q. Han, Appl. Phys. Lett. **88**, 1 (2006)
65. P. Kohler-Redlich, F. Ernst, M. Rühle, Chem. Mater. **11**, 3620 (1999)
66. J. Wei, B. Jiang, Y. Li, C. Xu, D. Wu, B. Wei, Straight boron carbide nanorods prepared from carbon nanotubes. J. Mater. Chem. **12**, 3121–3124 (2002)
67. M. Renzhi, Y. Bando, Chem. Phys. Lett. **364**, 314 (2002)
68. H.K. Clark, J.L. Hoard, The crystal structure of boron carbide. J. Am. Chem. Soc. **65**, 2115–2119 (1943)
69. V. Domnich, S. Reynaud, R.A. Haber, M. Chhowalla, Boron carbide: structure, properties, and stability under stress. J. Am. Ceram. Soc. **94**, 3605–3628 (2011)
70. A. Prakash, K.B. Sundaram, Optical studies of reactively Co-sputtered BCN thin films. ECS Trans. **61**, 51–56 (2014)
71. Y. Xian, R. Qiu, X. Wang, P. Zhang, Interfacial properties and electron structure of Al/B 4 C interface: a first-principles study. J. Nucl. Mater. **478**, 227–235 (2016)
72. T.V. Hynes, M.N. Alexander, Nuclear magnetic resonance study ofβ-rhombohedral boron and boron carbide. J. Chem. Phys. **54**, 5296–5310 (1971)
73. Thevenot F B 1974 **217**
74. Beckel L Mexico 1986 87131
75. M. Bouchacourt, F. Thevenot, The correlation between the thermoelectric properties and stoichiometry in the boron carbide phase B4C-B10.5C. J. Mater. Sci. **20**, 1237–1247 (1985)
76. J. Lee, H. Youn, K.S. Hong, Phase Transit., 83 (1999)
77. S. Ulrich, H. Ehrhardt, J. Schwan, R. Samlenski, R. Brenn, Subplantation effect in magnetron sputtered superhard boron carbide thin films. Diam. Relat. Mater. **7**, 835–838 (1998)
78. A.O. Sezer, J.I. Brand, Chemical vapor deposition of boron carbide. Mater. Sci. Eng. B **79**, 191–202 (2001)
79. S. Vepřek, S. Rambert, M. Heintze, F. Mattenberger, M. Jurčik-Rajman, W. Portmann, et al., J. Nucl. Mater. **162–164**, 724 (1989)
80. D. Byun, B.R. Spady, N.J. Ianno, P.A. Dowben, Comparison of different chemical vapor deposition methodologies for the fabrication of heterojunction boron-carbide diodes. Nanostructured Mater. **5**, 465–471 (1995)
81. Winter J, Esser H G, Reimer H, Grobusch L, Von Seggern J and Wienhold P 1990. J. Nucl. Mater. 176–177 486
82. S. Lee, J. Mazurowski, W.L. O'Brien, Q.Y. Dong, J.J. Jia, T.A. Callcott, Y. Tan, K.E. Miyano, D.L. Ederer, D.R. Mueller, P.A. Dowben, The structural homogeneity of boron carbide thin films fabricated using plasma-enhanced chemical vapor deposition from B5H9+CH4. J. Appl. Phys. **74**, 6919–6924 (1993)
83. D. Byun, S.D. Hwang, P.A. Dowben, F.K. Perkins, F. Filips, N. Ianno, J 1994. Appl. Phys. Lett. **64** (1968)
84. F.K. Perkins, R.A. Rosenberg, S. Lee, P.A. Dowben, Synchrotron-radiation-induced deposition of boron and boron carbide films from boranes and carboranes: Decaborane. J. Appl. Phys. **69**, 4103–4109 (1991)
85. F.K. Perkins, M. Onellion, S. Lee, D. Li, J. Mazurowski, P.A. Dowben, Appl. Phys. A Mater. Sci. Process. **450**, 442 (1992)
86. U. Jansson, J.O. Carlsson, B. Stridh, S. Söderberg, M. Olsson, Chemical vapour deposition of boron carbides I: Phase and chemical composition. Thin Solid Films **172**, 81–93 (1989)
87. J.C. Oliveira, O. Conde, Deposition of boron carbide by laser CVD: a comparison with thermodynamic predictions. Thin Solid Films **307**, 29–37 (1997)
88. L.G. Vandenbulcke, Theoretical and experimental studies on the chemical vapor deposition of boron carbide. Ind. Eng. Chem. Prod. Res. Dev. **24**, 568–575 (1985)
89. L. Vandenbulcke, G. Vuillard, Composition and structural changes of boron carbides deposited by chemical vapour deposition under various conditions of temperature and supersaturation. J. Less-Common. Met. **82**, 49–56 (1981)
90. M. Olsson, S. Söderberg, B. Stridh, U. Jansson, J.O. Carlsson, Chemical vapour deposition of boron carbides II: morphology and microstructure. Thin Solid Films **172**, 95–109 (1989)

91. J. Rey, G. Male, P. Kapsa, J. Loubet, J. Rey, G. Male, et al., J. Phys. Coll., 50 (1989)
92. M. Ducarroir, C. Bernard, Thermodynamic domains of the various solid deposits in the B-C-H-Cl vapor system. J. Electrochem. Soc. **123**, 136 (1976)
93. S.V. Deshpande, E. Gulari, S.J. Harris, A.M. Weiner, Filament activated chemical vapor deposition of boron carbide coatings. Appl. Phys. Lett. **65**, 1757–1759 (1994)
94. V.L. Solozhenko, D. Andrault, G. Fiquet, M. Mezouar, D.C. Rubie, Synthesis of superhard cubic BC2N. Appl. Phys. Lett. **78**, 1385–1387 (2001)
95. A.Y. Liu, M.L. Cohen, Prediction of new low compressibility solids. Science **245**, 841–842 (1989)
96. A.Y. Liu, R.M. Wentzcovitch, M.L. Cohen, Atomic arrangement and electronic structure ofBC2N. Phys. Rev. B **39**, 1760–1765 (1989)
97. A. Lousa, J. Esteve, S. Muhl, E. Martínez, BCN thin films near the B 4 C composition deposited by radio frequency magnetron sputtering. Diam. Relat. Mater. **9**, 502–505 (2000)
98. H. Yokomichi, T. Funakawa, A. Masuda, Preparation of boron–carbon–nitrogen thin films by magnetron sputtering. Vacuum **66**, 245–249 (2002)
99. S. Nakao, T. Sonoda, K. Tsugawa, J. Choi, T. Kato, Effects of nitrogen gas ratio on composition and microstructure of BCN films prepared by RF magnetron sputtering. Vacuum **84**, 642–647 (2009)
100. V.O. Todi, B.P. Shantheyanda, R.M. Todi, K.B. Sundaram, K. Coffey, Optical characterization of BCN films deposited at various N2/Ar gas flow ratios by RF magnetron sputtering. Mater. Sci. Eng. B Solid-State Mater. Adv. Technol. **176**, 878–882 (2011)
101. J. Yue, W. Cheng, X. Zhang, D. He, G. Chen, Ternary BCN thin films deposited by reactive sputtering. Thin Solid Films **375**, 247–250 (2000)
102. T. Tavsanoglu, M. Jeandin, O. Addemir, Synthesis and characterisation of thin films in the B–C–N triangle. Surf. Eng. **32**, 755–760 (2016)
103. M. Lei, Q. Li, Z. Zhou, I. Bello, C. Lee, S. Lee, Characterization and optical investigation of BCN film deposited by RF magnetron sputtering. Thin Solid Films **389**, 194–199 (2001)
104. V.O. Todi, B.P. Shantheyanda, K.B. Sundaram, Influence of annealing on the optical properties of reactively sputtered BCN thin films. Mater. Chem. Phys. **141**, 596–601 (2013)
105. D.H. Kim, E. Byon, S. Lee, J.-K. Kim, H. Ruh, Thin Solid Films **447–448**, 192 (2004)
106. L. Liu, Y. Wang, K. Feng, Y. Li, W. Li, C. Zhao, Y. Zhao, Preparation of boron carbon nitride thin films by radio frequency magnetron sputtering. Appl. Surf. Sci. **252**, 4185–4189 (2006)
107. C. Zhuang, J. Zhao, F. Jia, C. Guan, Z. Wu, Y. Bai, X. Jiang, Tuning bond contents in B–C–N films via temperature and bias voltage within RF magnetron sputtering. Surf. Coatings Technol. **204**, 713–717 (2009)
108. L. Liu, Y. Zhao, Y. Tao, D. Yang, H. Ma, Y. Li, Effects of experimental parameters on composition of boron carbon nitride thin films deposited by magnetron sputtering. Appl. Surf. Sci. **253**, 439–443 (2006)
109. A. Prakash, V. Todi, K.B. Sundaram, S.W. King, Hardness studies of RF sputtered deposited BCN thin films. ECS Trans. **58**, 147–153 (2014)
110. A. Prakash, V. Todi, K.B. Sundaram, L. Ross, G. Xu, M. French, P. Henry, S.W. King, Investigation of the dielectric and mechanical properties for magnetron sputtered BCN thin films. ECS J. Solid State Sci. Technol. **4**, N3122–N3126 (2015)
111. A. Prakash, K.B. Sundaram, ECS J. Solid State Sci. Technol. **5**, 35 (2016)
112. A. Prakash, K.B. Sundaram, A.D. Campiglia, Photoluminescence studies on BCN thin films synthesized by RF magnetron sputtering. Mater. Lett. **183**, 355–358 (2016)
113. A. Prakash, K.B. Sundaram, J. Vac. Sci. Technol. B Nanotechnol. Microelectron. Mater. Process. Meas. Phenom. **34**, 40603 (2016)
114. A. Prakash, G. Skaria, K.B. Sundaram, Investigation on electrical properties of RF sputtered deposited BCN thin films. ECS Trans. **53**, 53–58 (2013)
115. A. Prakash, K.B. Sundaram, Deposition and XPS studies of dual sputtered BCN thin films. Diam. Relat. Mater. **64**, 80–88 (2016)
116. A. Essafti, E. Ech-chamikh, M. Azizan, Structural and chemical study of a-BC, a-CN, and a-BCN Thin films prepared by reactive RF sputtering*. Spectrosc. Lett. **41**, 57–63 (2008)
117. E.M. Fayyad, A.M. Abdullah, M.K. Hassan, A.M. Mohamed, G. Jarjoura, Z. Farhat, Recent advances in electroless-plated Ni-P and its composites for erosion and corrosion applications: a review. Emergent Mater. **1**, 3–24 (2018)
118. O.O. Fadiran, N. Girouard, J.C. Meredith, Pollen fillers for reinforcing and strengthening of epoxy composites. Emergent Mater. **1**, 95–103 (2018)
119. A. Nagaraj, D. Govindaraj, M. Rajan, Magnesium oxide entrapped polypyrrole hybrid nanocomposite as an efficient selective scavenger for fluoride ion in drinking water. Emergent Mater. **1**, 25–33 (2018)
120. M. Mrlik, P. Sobolciak, I. Krupa, P. Kasak, Light-controllable viscoelastic properties of a photolabile carboxybetaine ester-based polymer with mucus and cellulose sulfate. Emergent Mater. **1**, 35–45 (2018)
121. A. Popelka, P. Sobol, M. Mrlík, Z. Nogellova, I. Chodák, M. Ouederni, M.A. Al-Maadeed, I. Krupa, Foamy phase change materials based on linear low-density polyethylene and paraffin wax blends. Emergent Mater. **1**, 47–54 (2018)
122. D. Ponnamma, A. Erturk, H. Parangusan, K. Deshmukh, M.B. Ahamed, M.A. Al-Maadeed, Stretchable quaternary phasic PVDF-HFP nanocomposite films containing graphene-titania-SrTiO3 for mechanical energy harvesting. Emergent Mater. **1**, 55–65 (2018)
123. T. Meng, C. Yi, L. Liu, A. Karim, X. Gong, Enhanced thermoelectric properties of two-dimensional conjugated polymers. Emergent Mater. **1**, 67–76 (2018)
124. A. Janson, J. Minier-Matar, E. Al-Shamari, A. Hussain, R. Sharma, D. Rowley, S. Adham, Evaluation of new ion exchange resins for hardness removal from boiler feedwater. Emergent Mater. **1**, 77–87 (2018)
125. N. Abdullah, N. Yusof, A.F. Ismail, F.E.C. Othman, J. Jaafar, L.W. Jye, W.N.W. Salleh, F. Aziz, N. Misdan, Effects of manganese(VI) oxide on polyacrylonitrile-based activated carbon nanofibers (ACNFs) and its preliminary study for adsorption of lead(II) ions. Emergent Mater. **1**, 89–94 (2018)
126. E. Byon, M. Son, N. Hara, K. Sugimoto, Thin Solid Films **447–448**, 197 (2004)
127. Z.F. Zhou, I. Bello, M.K. Lei, K.Y. Li, C.S. Lee, S.T. Lee, Surf. Coat. Technol. **128**, 334 (2000)
128. T.-H. Tsai, T.-S. Yang, C.-L. Cheng, M.-S. Wong, Synthesis and properties of boron carbon nitride (BN:C) films by pulsed-DC magnetron sputtering. Mater. Chem. Phys. **72**, 264–268 (2001)
129. A. Prakash, K.B. Sundaram, Studies on electrical properties of RF sputtered deposited boron carbon nitride thin films. ECS J. Solid State Sci. Technol. **4**, N25–N29 (2015)
130. A. Prakash, S.D. Nehate, K.B. Sundaram, Boron carbon nitride based metal-insulator-metal UV detectors for harsh environment applications. Opt. Lett. **41**, 4249 (2016)